Similarities Between Spaceborne Active and Airborne Passive Microwave Observations at 1 km Resolution

Christoph Rüdiger, *Member, IEEE*, Marcela Doubková, Joshua R. Larsen, Wolfgang Wagner, *Senior Member, IEEE*, and Jeffrey P. Walker

***Abstract*—For the first time, airborne passive microwave data were collected at 1 km resolution over parts of Central Australia coinciding with spaceborne active data, allowing a comparison of such data sets acquired at medium (1 km) spatial resolution. L-band airborne passive microwave scenes were compared with C-band scenes and temporal parameters from the Advanced Synthetic Aperture Radar. It was found that the radar-returned signal, as well as the "sensitivity" and "correlation" parameters derived from the long time-series of the ASAR GM data, is similar to spatial patterns in the passive microwave data, suggesting that similar physical interactions are underlying both data sets, especially across heterogeneous landscapes. Comparable patterns found over the dry Lake Eyre salt bed ($r^2 = 0.37$) suggest that very high-resolution C-band radar data may be used to describe subpixel heterogeneity within coarse resolution radiometer data, such as the future Soil Moisture Active Passive mission.**

***Index Terms*—Disaggregation, environmental monitoring, microwave passive and active remote sensing, satellites, soil moisture.**

I. Introduction

Soil moisture plays a critical role in climate and weather prediction [1], and is also important in determining a catchment's runoff generation response to rainfall [2], [3]. It has also been determined as one of the Essential Climate Variables (ECV) necessary to characterize and model the climate of the Earth [4]. Remotely sensed soil moisture products have been derived from microwave sensors that have been operated since the late 1970 s [5]–[7], mostly at spatial resolutions in excess of 25 km resulting from limitations in the sensor's technology [7]–[9]. While this may be sufficient for many weather and climate forecast models, it does not cover the spatial resolution demand (< 5 km) of applications such as water management, flood forecasting or agriculture.

One way to retrieve soil moisture at finer spatial scales is to enhance the understanding of the subpixel surface responses of coarse resolution data, e.g., through downscaling. Methods for downscaling have been introduced for the Advanced Scatterometer (ASCAT) soil wetness product [10] and by the Soil Moisture Active Passive (SMAP) [11] and Soil Moisture and Ocean Salinity (SMOS) [12] teams. While [10] suggest that the high resolution patterns in soil moisture are essentially time-invariant and may be determined with high-resolution observations at any time, the SMAP aims to use coinciding medium resolution (3 km) active microwave data to downscale very accurate coarse resolution (36 km) passive microwave data at L-band, to deliver a 9 km product [13]. Based on the assumptions of [10], the launch of the Sentinel-1 mission in April 2014 (which is equipped with an active instrument operating at high spatial resolution of 5 m $\times$ 20 m), will potentially allow disaggregating any coarse-resolution microwave products to a previously not achievable spatial resolution. While a strong correlation was found within the temporal change in brightness temperature and radar [14], a downscaling algorithm for SMAP was developed and tested with SMEX02 data [11], [15]. Similarly, good correlations were found between coinciding L-band radiometer and radar signals for four different airborne campaigns [16] using the Passive and Active L-band System (PALS) [17]. However, those studies were undertaken utilizing coinciding airborne passive and active observations at L-band. To implement future Sentinel-1 C-band data for the disaggregation of the data from L-band radiometers such as the SMOS [7] and SMAP [13] missions, the relationship between L-band brightness temperature and C-band backscatter data must be determined at comparable resolutions, and forms the basis of the work presented here.

This letter provides an insight into the relationship of different medium-resolution microwave data by comparing the spaceborne C-band Advanced Synthetic Aperture Radar on board ENVISAT with the airborne Polarimetric L-band Multibeam Radiometer (PLMR) [18] across parts of the Australian Arid Zone. The major innovation lies in the use of both passive and active systems for subpixel understanding of coarse scale passive microwave products based on the hypothesis that both

Manuscript received January 8, 2014; revised May 5, 2014; accepted May 10, 2014. Christoph Rüdiger and flights of the arid zone field campaigns were supported by an Australian Research Council Discovery Project grant (DP0879212). PLMR was funded by an ARC Linkage Infrastructure, Equipment and Facilities grant (LE0453434) The ASAR data were made available through a project partly funded by ESA SHARE-Extension2 project (ESRIN/ Contract No.19420/05/I-EC).

C. Rüdiger and J. P. Walker are with the Department of Civil Engineering, Monash University, Clayton, VIC 3800, Australia.

M. Doubková is with the Department of Geodesy and Geoinformation, Vienna University of Technology, Austria and she was also with European Space Agency, ESRIN, 00044 Frascati, Italy.

J. R. Larsen is with the School of Geography. Planning, and Environmental Management, University of Queensland, Brisbane, Qld 4072, Australia.

W. Wagner is with the Department of Geodesy and Geoinformation, Vienna University of Technology, 1040 Vienna, Austria.

Color versions of one or more of the figures in this paper are available online at http://ieeexplore.ieee.org.

Digital Object Identifier 10.1109/LGRS.2014.2323712

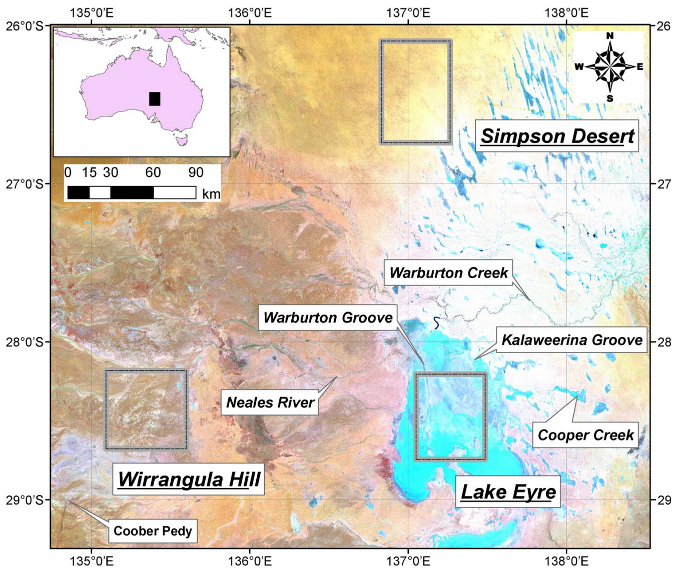

Fig. 1. Location of the field sites (grey boxes) across the Australian Arid Zone overlain on a Landsat image (insert: location of the Australian Arid Zone study area).

active and passive data principally deal with the same physical surface phenomena [19]. The question of interest is whether the radar backscatter signal of the active microwave satellite contains the information of the spatial patterns that are required for the downscaling of passive emissions at L-band. The studied region includes three different landscape classes (sandy desert, rocky desert pavement and a salt lake), all with minimal vegetation. Particular focus is paid to the spatial patterns observed over Lake Eyre, Australia's largest salt lake with an extensive salt crust that is subject to rare flooding events.

II. Data Sets

A. Radiometer Brightness Temperature

The airborne passive microwave data were collected during the southern hemisphere summer (November 2008) and winter (August 2009) through the SMOS Arid Zone Experiments (SAZE-Oz) for the purpose of assessing potential passive microwave calibration targets at L-band in Australia [20]. The study area (Fig. 1) covers the central Australian arid zone with very dry conditions throughout the year ($< 100 - 200$ mm/yr) and only occasional precipitation events. As a result, both campaigns represented dry conditions but for different seasons (i.e., the temperature regimes of winter and summer). The study area is located between $26° - 29°$ S and $135° - 137.5°$ E containing highly contrasting surface conditions ranging from a large salt playa (Lake Eyre), through a sandy desert with up to 20 m high dunes with an average spacing of 400 m (Simpson Desert), to a large expanse of stony desert pavement (Wirrangula Hill).

The instrument deployed on the aircraft is the Polarimetric L-band Multibeam Radiometer (PLMR), operating at a frequency of 1.413 GHz (± 12 MHz) [18] and was flown in pushbroom configuration at an altitude of 3000 m above ground level, resulting in a swath width of 6 km (six beams at $\sim$1 km resolution) and an along track sampling rate of $\sim$40 m at operational flight velocities ($\sim$140 knots). For each field site and campaign, an area of ~ 50 km $\times$ 50 km was covered. The flights used in the present study took place on the 10th (Lake Eyre) and 12th of November 2008 (Wirrangula Hill), and 11th of August 2009 (Simpson Desert). The PLMR data were corrected for diurnal temperature changes during the five-hour-long 6 A.M.-centered flights using ground-based in situ monitoring stations. The data were also normalized to a reference angle of 38°, which is close to the ASAR reference incidence angle of 40°. For PLMR, the normalization error was found to be in the order of 2.64 K (h-pol) and 0.93 K (v-pol). A full description of the PLMR post-processing is contained in [20], [21].

B. Radar Backscatter

The radar backscatter information was retrieved from the Advanced Synthetic Aperture Radar (ASAR) onboard ENVISAT in its Global Mode (GM) operations, collected during its overpass on 9th of November 2008, 0100 UTC ($\sim$20 hrs prior to the PLMR flights over Lake Eyre), and 8th of August 2009 ($\sim$56 hrs prior to the flight). The Global Monitoring (GM) mode operated at the spatial resolution of 1 km across a 400 km wide swath and was in principle able to monitor each location on the Earth every 2 to 4 days. The ASAR GM data have been processed at the Vienna University of Technology (TU Wien) using their SAR processing chain [22], [23]. It consists of the steps geocoding, radiometric correction, resampling, normalisation, and soil wetness retrieval.

In addition to the backscatter scenes, two ASAR GM parameters derived from the long time-series of data were analyzed for their correspondence to the PLMR data:

- spatio-temporal coherence computed as a correlation in time between ASAR GM normalized backscatter on a local (1 km) and regional (25 km) scale;
- sensitivity computed as the difference between the historically highest and lowest backscatter values.

These long-term parameters have proved to be beneficial for the interpretation of coarse resolution data [10] and may provide information on land cover, topography, and long-term variability of the soil hydric state. More detailed descriptions of these parameters can be found in [24], [27]. [27] also discussed the quantification of the normalization error, and found that it can be expressed as a function of noise around the slope parameter and the local incidence angle.

III. Results and Discussions

A. Spatial Patterns (Qualitative Analysis)

A qualitative comparison of the spatial patterns of brightness temperature from PLMR and the Advanced Microwave Scanning Radiometer for the Earth Observing System (AMSR-E), as well as backscattering coefficient from ASAR GM is shown in Fig. 2. It is evident that the coarse scale resolution passive microwave data of AMSR-E [Fig. 2(a)] contain a lower level of detail comparable to the other three products [Fig. 2(b)–(d)]. Moreover, some mixed-pixel response appears in the AMSR-E pixels surrounding Lake Eyre as a consequence of the relatively

This article has been accepted for inclusion in a future issue of this journal. Content is final as presented, with the exception of pagination.

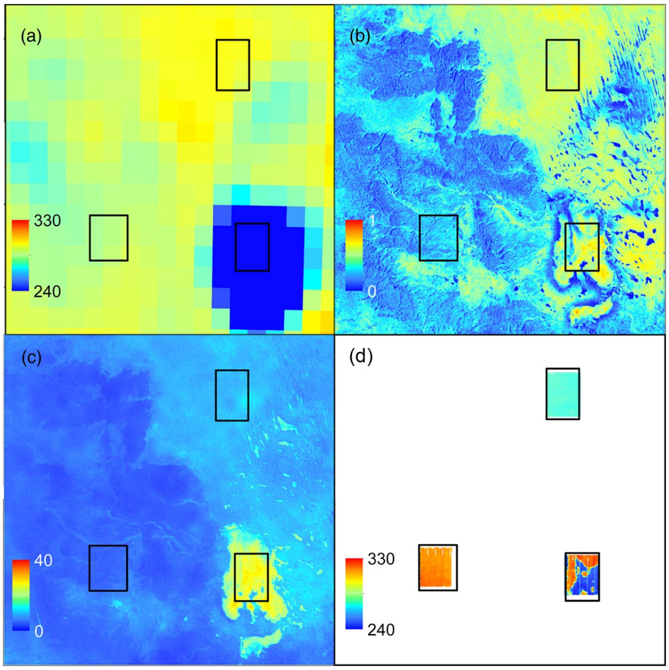

Fig. 2. Spatial distribution of (a) AMSR-E brightness temperatures [K] at horizontal polarization (11 November 2008), (b) ASAR correlation layer, (c) ASAR sensitivity layer [σ], and (d) PLMR brightness temperature [K] data (horizontal polarization) for the SAZE-Oz domain at their respective resolutions. Note that PLMR and AMSR-E plots have the same color scale and that the PLMR data are from the following dates: 10 November 2008 (Lake Eyre), 12 November 2008 (Wirrangula Hill), and 11 August 2009 (Simpson Desert).

large AMSR-E footprint. Despite this, the large-scale patterns (25–50 km) are detected by both, the ASAR GM and the AMSR-E data. For instance, the Simpson Desert in the far north of the study area has consistently high values in the ASAR GM *correlation* [Fig. 2(b)] and *sensitivity* data [Fig. 2(c)] as well as higher brightness temperatures in the AMSR-E and PLMR data. Similarly, Lake Eyre is discernible in the ASAR GM *sensitivity* layer, due to the hydrological variability of the lake's surface and shallow subsurface, as well as in the AMSR-E and PLMR data with its lower brightness temperature values, due to the high soil moisture and salinity contents of the soil.

The spatial variability is low in both, PLMR and ASAR scenes across the sandy Simpson Desert and the Wirrangula Hill desert pavements. Also, a decreasing north-east to south-west gradient over the Wirrangula Hill is evident in both scenes. This suggests that both sensors are sensitive to the same surface characteristics. However, the absence of distinct patterns over the Simpson Desert makes validation of this hypothesis difficult, since no further actual landscape effects can be correlated between the data sets.

In contrast to the dune field and stony desert areas, Lake Eyre exhibits strong spatial patterns that appear in both the ASAR GM and PLMR data and reflect the varying surface and moisture conditions. The surface conditions at any one time are largely driven by the lake's bathymetry (resulting in different moisture conditions depending on the depth of the groundwater), density and thickness of the salt crust, surface water depth, and clay content [25], [26]. These factors are also related to the distribution of water and sediment from Warburton Creek (the largest tributary to the lake) which enters the lake from the north-east, as well as the low relief Warburton Groove within the lake itself (Fig. 1). Occasionally (every 5–10 years), Lake Eyre also receives runoff input from other tributaries such as the Neales River to the west and the Cooper Creek to the east, however, those rivers have a far smaller sediment load and therefore do not impact the soil conditions of Lake Eyre as significantly as the Warburton Creek. Due to the higher discharge and sediment load of the Warburton Creek, high clay content is expected around the extensive delta developed by the Warburton Creek. During lower flood stages, the northern parts of the lake can be bypassed and water transported directly to the center and southern portions of the lake via the Warburton and Kalaweerina Grooves, which are clearly distinguishable as the extended area of warmer passive microwave emissions and increased backscatter values running from north to south and almost covering the entire western section of Lake Eyre (Fig. 2). This bypassing of water flows results in an uneven distribution of halite (or rock salt), clay and surface water across the playa surface.

Despite the many similarities between the PLMR and ASAR GM data across the study area, some important differences were also evident within the central-southern sections of Lake Eyre. Here, the ASAR GM backscatter indicates significantly higher than average values. On the contrary, the PLMR brightness temperatures are rather low suggesting occurrence of wet or saline soils. This discrepancy may be attributed to rapid changes in surface conditions between the PLMR and ASAR GM acquisitions (PLMR data having been acquired one day later) that may include changes in daily soil moisture, temperature or influence of wind on surface water depth. Also, the discrepancies may be due to the different observation depths of the two sensors and consequent effects of the humid salty crusts and underlying saturated soils. In particular, while the saturated soils introduce a significant lowering effect on the longer wavelength L-band brightness temperatures, the salty crusts highly increase the ASAR GM C-band backscatter. This occurs, as the rougher surface conditions of the crust cannot be penetrated by the shorter wavelength of the C-band sensor. As a result, the C-band cannot observe the soil water beneath the crust. Interestingly, the thickness of the salt crust has been noted to be centimeters thick in areas that are frequently inundated, but may reach in excess of 40 cm in the south-western parts of the lake [25]. Over these areas the effect of wind can be particularly strong.

On the basis of the above results, it is suggested that the deeper observation depth of the L-band radiometer corresponds to subsurface saturation of this section of the lake bed, as opposed to the C-band radar which is more heavily influenced by conditions close to the surface, and possible volume scattering of the radar signal within the relatively dry salt crust.

B. *Spatial Patterns (Quantitative Analysis)*

Fig. 3 (top row) quantifies the correspondence between brightness temperatures and backscatter across the three sites. To limit the noise in the ASAR GM data and for a better comparison, both data sets were aggregated onto an identical, regular 2 km grid. The coefficient of determination using a

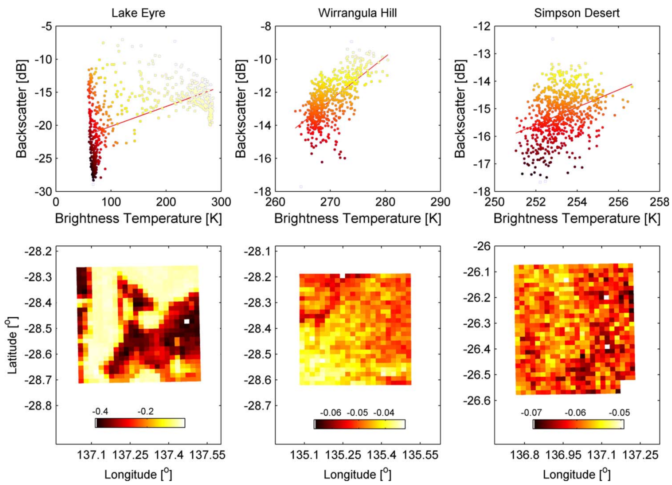

Fig. 3. Scatterplots of horizontally polarized brightness temperature [K] and hh-polarized backscatter [σ] data (top row) across the three study sites (note the different scales between the plots); and spatial distribution of the function dB/K (bottom row). The colors are a function of $f_{\mathrm{rel}}(1)$.

TABLE I
OVERVIEW OF THE COEFFICIENT OF DETERMINATION (r^2) OF A SECOND-ORDER POLYNOMIAL REGRESSION BETWEEN THE BRIGHTNESS TEMPERATURES AND BACKSCATTER ACROSS THE THREE STUDY SITES

Site	*r^2*
Lake Eyre	0.29
Wirrangula Hill	0.41
Simpson Desert	0.13

second-order polynomial least-squares regression is presented in Table I. All three sites appear to have significantly different response types in the active and passive signals. The highly varying data across Lake Eyre results in a nonlinear relationship with an apparent saturation at high brightness temperatures. To better identify the relationship between the backscatter and the brightness temperature a relative function, f_{rel}, is introduced

$$f_{rel} = \frac{dB}{K} \tag{1}$$

where dB and K are the ASAR GM radar backscatter and the PLMR passive brightness temperatures, respectively. This function highlights the nonlinear relationship between backscatter and brightness temperatures and intensifies the spatial patterns across the field sites (Fig. 3). Throughout Lake Eyre, the values with high backscatter, but low brightness temperatures are mainly found in the transitional zones along the Warburton Groove, and also along the playa to the north east. The coefficient of correlation is improved to 0.37 when removing those areas, which consist mainly of mixed pixel areas and where an interaction between clay crust, salt and rising subsurface water yield different responses in the two data sets.

Contrastingly, the two dry locations (Simpson Desert and Wirrangula Hill) display a behavior that is closer to a linear relationship (Fig. 3). The low coefficient of determination for the Simpson Desert is a consequence of the low spatial variability (0.7 K and 1.1 dB), which for both sensors is at or below the observation accuracy of the sensors themselves, and therefore is not significant. The data across Wirrangula Hill (stony desert pavement), however, shows a near linear relationship ($r^2 = 0.41$). Both data sets have the same south-west to north-east gradient, and appear to have a similar response along the sparsely vegetated area along the river in the north-west corner of the field site, which may be used to identify hydrologically active areas within desert environments.

C. Long-Term Backscatter Patterns

The long-term patterns were studied using statistics derived from the long time-series of the ASAR GM data. Computed as the difference between the historically lowest and highest backscatter coefficients, the ASAR GM *sensitivity* layer accounts for the temporal dynamics of the target [27], while the ASAR GM *correlation* parameter represents the spatial coherence of a single pixel relative to its region (25 km).

A high sensitivity ($\sim$25 dB) in the ASAR backscatter data was found mainly across the southern sections of Lake Eyre [Fig. 2(c)], a result of episodic flooding events, and the subsequent evaporation and infiltration of the water that leaves the lake surface completely dry. Correspondingly, flood plains are visible just north of Lake Eyre (reflected by higher brightness temperature and backscatter), where water is collected after strong precipitation events. This episodic flooding did not significantly affect the northern parts or the Warburton Groove ($\sim$10 dB). In combination with the high brightness temperatures in the area, this suggests that subsurface flows dominate in this area, rather than surface floods, with the exception of the very center of the Warburton Groove, which displays lower brightness temperatures and lower *correlation/sensitivity*. The areas just north of Lake Eyre, also extending into the eastern parts of the Simpson Desert, display a similarly high sensitivity, which can be attributed to intermittent flooding and seepage into the clay pans. Conversely, the sandy desert areas of the Simpson Desert in the north east and the desert pavement surfaces of the area around Wirrangula Hill display significantly lower temporal variability (Fig. 2(c); 3–10 dB), which is consistent with the low hydrological activity at those sites.

Several areas in the Wirrangula Hill region have a significantly lower correlation (0.1) value when compared to their neighboring pixels (0.5) [Fig. 2(b)]. It is assumed that the very rough surface and small topographical features of Wirrangula Hill have only little temporal dynamics and therefore do not display a high coherence with their surrounds. The characteristics of the backscatter coefficient may then differ significantly in time mainly due to signal noise, causing the low correlation. Since a high coherence is generally the result of a non-negligible temporal variability in the signal, it can be argued that the areas with coherence close to 0 (such as Wirrangula Hill) are well suited for vicarious calibrations, which supports the findings of [20].

IV. DISCUSSION AND CONCLUSION

A high correspondence between the spatial patterns of the C-band ASAR GM backscatter and airborne L-band PLMR brightness temperature observations was demonstrated at 1 km resolution. Similarly, a good qualitative correspondence was demonstrated also with coarse resolution AMSR-E brightness temperature data. Nevertheless, the AMSR-E contained much lower level of detail comparable to the other data. However, the results also suggest that issues may arise when using high-resolution backscatter data to downscale radiometer data within a coarse resolution pixel (e.g., in the context of SMAP) due to significantly different response types for the varying surface conditions. This in turn suggests that more physically based downscaling methodologies such as DisPATCh [12] may also be used alongside the backscatter information, to better inform the algorithm of the surface conditions. The normalization errors as discussed above will not affect the downscaling results, as they do not affect the mean observation.

The results of this letter demonstrate that the high-resolution radar backscatter data (such as the past Envisat ASAR and the recently launched Sentinel-1 instruments) contain information also seen by their passive counterparts and thus offer the possibility for disaggregation of lower resolution passive observations and to achieve more accurate higher resolution data products. This suggests that the future SMAP mission, which proposes to use medium resolution L-band microwave instruments onboard the same satellite to downscale low resolution radiometer observations to 3 km, can potentially use other higher resolution products at C-band to achieve an even better spatial resolution.

It was also found that the use of long-term statistics from ASAR GM data may provide additional information on the spatial structure within the area. This will help to overcome radiometric quality issues of the data through temporal smoothing. However, it remains to be seen whether the full data series information should be used or if only a limited time series is required.

Finally, the detection of the spatial patterns across Lake Eyre, as well as their apparent temporal stability have some significant implications for the interpretation of hydrologic effects across Lake Eyre and in the southern areas of the Simpson Desert. The presented capacity to detect water saturated as well as dry soil at this resolution allows unprecedented insights into the hydrology of Lake Eyre and other remote regions with no hydrological monitoring. While the clay pans developed within the lake from the Warburton Creek inflow can clearly be distinguished, future applications of these information will include tracking the progression of subsurface water along Lake Eyre and its tributaries, as well as the detection, extent and timing of the seepage areas along its margins.

Acknowledgment

The authors would like to thank all participants of the two campaigns, in particular A. Marks and J. Johanson.

References

[1] S. I. Seneviratne *et al.*, "Investigating soil moisture -climate interactions in a changing climate: A review," *Earth-Sci. Rev.*, vol. 99, no. 3/4, pp. 125–161, May 2010.

[2] J. Parajka *et al.*, "Seasonal characterstics of flood regimes across the Alpine-Carpathian range," *J. Hydrol.*, vol. 394, no. 1/2, pp. 78–89, Nov. 2010.

[3] V. Sheikh, E. Van Loon, R. Hessel, and V. Jetten, "Sensitivity of LISEM predicted catchment discharge to initial soil moisture content of soil profile," *J. Hydrol.*, vol. 393, no. 3/4, pp. 174–185, Nov. 2010.

[4] "Implementation plan for the global observing system for climate in support of the UNFCCC," Geneva, Switzerland, Tech. Rep. GCOS-138, 2010.

[5] Z. Bartalis *et al.*, "Initial soil moisture retrievals from the METOP-A Advanced Scatterometer (ASCAT)," *Geophys. Res. Lett.*, vol. 34, no. 20, p. L20401, Oct. 2007.

[6] M. Owe, R. de Jeu, and T. Holmes, "Multisensor historical climatology of satellite-derived global land surface moisture," *J. Geophys. Res.—Earth Surface*, vol. 113, no. F1, p. F01002, 2008.

[7] Y. H. Kerr *et al.*, "The SMOS mission: New tool for monitoring key elements of the global water cycle," *Proc. IEEE*, vol. 98, no. 5, pp. 666–687, May 2010.

[8] E. G. Njoku, T. J. Jackson, V. Lakshmi, T. K. Chen, and S. V. Nghiem, "Soil moisture retrieval from AMSR-E," *IEEE Trans. Geosci. Remote Sens.*, vol. 41, no. 2, pp. 215–229, Feb. 2003.

[9] L. Li *et al.*, "WindSat global soil moisture retrieval and validation," *IEEE Trans. Geosci. Remote Sens.*, vol. 48, no. 5, pp. 2224–2241, May 2010.

[10] W. Wagner *et al.*, "Temporal stability of soil moisture and radar backscatter observed by the Advanced Synthetic Aperture Radar (ASAR)," *Sensors*, vol. 8, no. 2, pp. 1174–1197, 2008.

[11] N. N. Das, D. Entekhabi, and E. G. Njoku, "An algorithm for merging SMAP radiometer and radar data for high resolution soil moisture retrieval," *IEEE Trans. Geosci. Remote Sens.*, vol. 49, no. 5, pp. 1504–1512, May 2011.

[12] O. Merlin *et al.*, "Disaggregation of SMOS soil moisture over the AACES area with DisPATCh," *IEEE Trans. Geosci. Remote Sens.*, vol. 50, no. 5, pp. 1556–1571, May 2011.

[13] D. Entekhabi *et al.*, "The Soil Moisture Active Passive (SMAP) mission," *Proc. IEEE*, vol. 98, no. 5, pp. 704–716, May 2010.

[14] U. Narayan, V. Lakshmi, and T. J. Jackson, "High-resolution change estimation of soil moisture uising L-band radiometer and radar observations made during the SMEX02 experiments," *IEEE Trans. Geosci. Remote Sens.*, vol. 44, no. 6, pp. 1545–1554, Jun. 2006.

[15] N. N. Das *et al.*, "Tests of the SMAP combined radar and radiometer algorithm using airborne field campaign observations and simulated data," *IEEE Trans. Geosci. Remote Sens.*, vol. 52, no. 4, pp. 2018–2028, Apr. 2014.

[16] A. Colliander, "Analysis of coincident L-band radiometer and radar measurements with respect to soil moisture and vegetation conditions," *Eur. J. Remote Sens.*, vol. 45, no. 1, pp. 111–120, 2012.

[17] W. J. Wilson *et al.*, "Passive Active L- and S-band (PALS) microwave sensor for ocean salinity and soil moisture measurements," *IEEE Trans. Geosci. Remote Sens.*, vol. 39, no. 5, pp. 1039–1048, May 2001.

[18] R. Panciera *et al.*, "The NAFE'05/CoSMOS Dataset: Towards SMOS soil moisture retrieval, downscaling and assimilation," *IEEE Trans. Geosci. Remote Sens.*, vol. 46, no. 3, pp. 736–745, Mar. 2008.

[19] E. Schanda, *Physical Fundamentals of Remote Sensing*. Berlin, Germany: Springer-Verlag, 1986.

[20] C. Rüdiger *et al.*, "Towards vicarious calibration of microwave remote sensing satellites in arid environments," *IEEE Trans. Geosci. Remote Sens.*, vol. 52, no. 3, pp. 1749–1760, Mar. 2014.

[21] C. Rüdiger, J. P. Walker, and Y. H. Kerr, "On the Airborne spatial coverage requirement for microwave satellite validation," *IEEE Geosci. Remote Sens. Lett.*, vol. 8, no. 4, pp. 824–828, Jul. 2011.

[22] M. Doubková, A. J. I. M. Van Dijk, D. Sabel, W. Wagner, and G. Blöschl, "Evaluation of the predicted error of the soil moisture retrieval from C-band SAR by comparison against modelled soil moisture estimates over Australia," *Remote Sens. Environ.*, vol. 120, no. 2, pp. 188–196, May 2012.

[23] D. Sabel, Z. Bartalis, W. Wagner, M. Doubková, and J. P. Klein, "Development of a global backscatter model in support to the sentinel-1 mission design," *Remote Sens. Environ.*, vol. 120, pp. 102–112, May 2012.

[24] D. Sabel, M. Doubková, W. Wagner, P. Snoeij, and E. Attema, "A global backscatter model for C-band SAR," in *Proc. ESA Living Planet Symp.*, Bergen, Norway, Jul. 2010, pp. 1–5.

[25] J. A. Dulhunty, "Salt crust distribution and lake bed conditions in southern areas of Lake Eyre North," *Trans. R. Soc. South Aust.*, vol. 98, no. 3, pp. 125–133, 1974.

[26] South Australia Engineering and Water Supply Dept., 99 p V. Kotwicki, Floods of Lake Eyre, Adelaide, Australia 1986, 99 p.

[27] C. Pathe, W. Wagner, D. Sabel, M. Doubková, and J. B. Basara, "Using ENVISAT ASAR global mode data for surface soil moisture retrieval over OK, USA," *IEEE Trans. Geosci. Remote Sens.*, vol. 47, no. 2, pp. 468–480, Feb. 2009.